Title
High-resolution second-harmonic optical coherence tomography of collagen in rat-tail tendon

Journal
Applied Physics Letters, 86(13)

ISSN
0003-6951

Authors
Jiang, Yi
Tomov, Ivan V
Wang, Yimin
et al.

Publication Date
2005-03-28

DOI
10.1063/1.1894607

High-resolution second-harmonic optical coherence tomography of collagen in rat-tail tendon

Yi Jiang, Ivan V. Tomov, Yimin Wang, and Zhongping Chen[a)]
Beckman Laser Institute and Department of Biomedical Engineering, University of California, Irvine, Irvine, California 92612

(Received 6 December 2004; accepted 23 February 2005; published online 22 March 2005)

A high-resolution second-harmonic optical coherence tomography (SH-OCT) system is demonstrated using a spectrum broadened femtosecond Ti:sapphire laser. An axial resolution of 4.2 μm at the second-harmonic wave center wavelength of 400 nm has been achieved. Because the SH-OCT system uses the second-harmonic generation signals that strongly depend on the orientation, polarization, and local symmetry properties of chiral molecules, this technique provides unique contrast enhancement to conventional optical coherence tomography. The system is applied to image biological tissues of the rat-tail tendon. Highly organized collagen fibrils in the rat-tail tendon can be visualized in recorded images. © *2005 American Institute of Physics*.
[DOI: 10.1063/1.1894607]

Optical coherence tomography (OCT) is an emerging imaging technology that provides *in vivo* high-resolution, cross-sectional images of biological tissues.[1] Using coherence gating technique, OCT is capable of detecting the backscattered light from highly scattering tissues at depths of 1–3 mm.[2] OCT imaging contrast originates from the inhomogeneities of sample scattering properties that are linear dependent on sample refractive indices. In many instances, such as pathological processes in tissue, changes in sample linear scattering properties are small and difficult to measure. For example, many cancers originate in the epithelium that has a thickness suitable for OCT imaging, but in their early stages when these cancers are developing through cell dysplasia, changes in tissue morphology and refractive index between normal and diseased tissues are very small and difficult to detect. Therefore, to meet the challenges found in OCT clinical applications, imaging contrast enhancement is very important. In recent years, many OCT contrast enhancement methods have been developed. These techniques include Doppler OCT,[3] polarization sensitive OCT,[4] spectroscopic OCT,[5] and administration of contrast agents for OCT.[6] More recently, using the nonlinear optical effect of second-harmonic generation (SHG)[7,8] for OCT contrast enhancement has also been demonstrated.

SHG is a powerful contrast mechanism in nonlinear optical microscopy. SHG signals provide unique information regarding sample structure symmetry because signals strongly depend on the orientation, polarization and local symmetry properties of chiral molecules.[9] SHG enables direct imaging of anisotropic biological structures, such as membranes, structure proteins, and microtubule ensembles. In addition to successfully producing high-resolution, high contrast images of tissue morphology,[10,11] recently SHG microscopy has also been applied to study dynamics in tissue physiology, such as monitoring collagen modification in tumor growth,[12] and optically recording action potential change in neuron cells.[13] SHG is emerging as a powerful nonlinear optical imaging modality for cell biology and biophysics.

In this letter, we demonstrate a high-resolution second-harmonic optical coherence tomography (SH-OCT) system. Using broadband, pulsed laser illumination and nonlinear interferometry, the system combines the molecular structure sensitivity of SHG with the coherence gating of OCT. Due to the decoupling of the axial and transverse scans, two-dimensional cross-sectional images of anisotropic biological structures can be obtained through one-dimensional scanning of the sampling beam, which has the potential to be adapted to clinic endoscopic studies. The light source utilized in this study is a spectrum broadened femtosecond Ti:sapphire laser. The sample under illumination generates SHG signal. Reference SHG signal is generated by a nonlinear crystal. Coherence gating detection of these SHG signals produces interference fringes that can be used for image construction. The current system achieves an axial imaging resolution of 4.2 μm in free space, corresponding to 3.1 μm in tissue, which is a sixfold improvement over the system we demonstrated previously.[7] The SH-OCT system is applied to image the biological tissue of a native, intact rat-tail tendon, and produces high contrast, high-resolution images detailing the collagen fibril organization within tendon tissue.

Figure 1 shows a schematic of the experimental setup. The Ti:sapphire laser generates 170 fs pulses at a wavelength of 800 nm with a repetition rate of 76 MHz. The femtosecond pulses are coupled into a 2.0-m-long high numerical aperture single mode fiber (Corning HI-780) for spectrum broadening. The OCT system consists of a Michelson interferometer illuminated by the continuum generated from the fiber. A broadband, nonpolarization beamsplitter is used to support interference fringes at both the fundamental and SH wavelengths. In the sample arm the beam is focused on the sample through a microscope objective. Backscattered fundamental and SH waves from the sample are collected by the same excitation objective. In the reference arm, the SH wave is generated when the laser beam passes through a thin β-BaB_2O_4 (BBO) nonlinear crystal. The beam then reflects back from a dichroic mirror mounted on a piezoelectric actuator. The dichroic mirror reflects 90% of the SH wave and 5% of the fundamental wave. A prism pair made from BK7 glass is inserted into the reference arm to compensate for the

a)Electronic mail: zchen@laser.bli.uci.edu

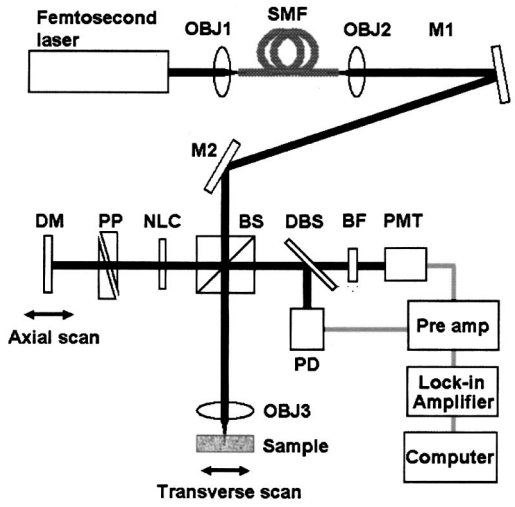

FIG. 1. High resolution SH-OCT experimental setup: (OBJ1-OBJ3) objectives; (SMF) single mode fiber; (M1-M2) mirrors; (BS) broadband nonpolarization beam splitter; (NLC) nonlinear crystal BBO; (PP) prism pair dispersion compensator; (DM) dichroic mirror; (DBS) dichroic beam splitter; (PD) photodiode; (BF) band-pass filter; (PMT) photomultiplier tube.

group velocity mismatch in the two arms. Because material dispersion of the optical components is not uniform for all the wavelengths, the fundamental and SH waves require different thicknesses of compensating material to generate optimized fringes at corresponding wavelengths. In the detection arm, a dichroic beamsplitter is used to separate the beam according to the wavelength. Fundamental and SH interference fringes are detected by a photodiode and a photomultiplier, respectively. A band-pass filter centered at 400 nm with 40 nm bandwidth is attached to the photomultiplier head to reject background noise. The coherence point spread functions of the presented system at fundamental and second-harmonic wavelengths are shown in Figs. 2(c) and 2(d). Measured in free space, the fundamental wave has a coherence length of 6.0 μm and the SH wave has a coherence length of 4.2 μm, which determine the axial resolutions of the OCT system at corresponding wavelengths.

Rat-tail tendon was chosen for the imaging experiment since many of its important properties are known from other

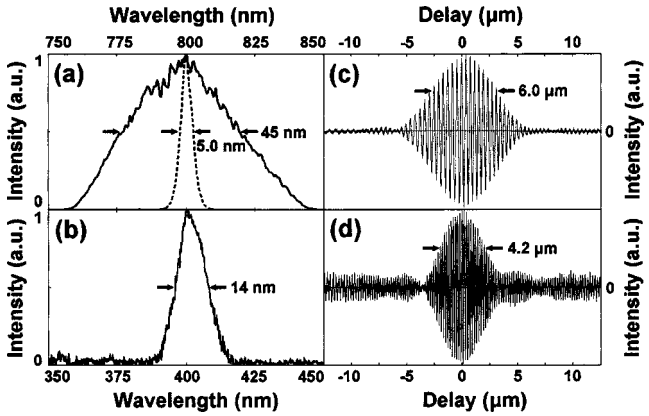

FIG. 2. Coherence length measurements: (a) spectrum of the fundamental wave. The dashed curve is the original spectrum of the laser, and the solid curve is the spectrum of the continuum generated from the fiber; (b) spectrum of the SH wave from the nonlinear crystal; (c) coherence point spread function of the fundamental wave, showing a coherence length of 6.0 μm; (d) coherence point spread function of the SH wave, showing a coherence length of 4.2 μm.

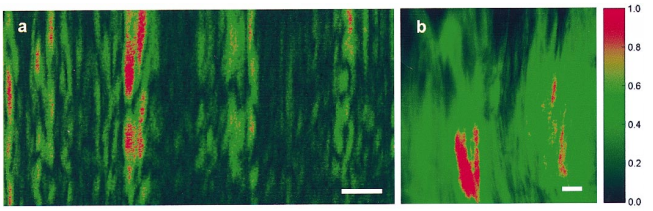

FIG. 3. (Color) (a) SH-OCT image showing an area of 100×50 μm in the rat-tail tendon, where many cable-like, parallel oriented, and slightly wavy collagen fiber bundles (fascicles) can be visualized; (b) 60X polarization microscope image of the same sample (scale bar: 10 μm).

independent methods.[14] Collagen is the most abundant protein in higher vertebrates, comprising over one-third of total body protein and 60%–86% of the dry weight of a tendon. Other components of tendons include water, proteoglycans, cells, elastin, and other extracellular matrix components. All of these components are arranged in a fibrous structure, as shown in the 60× polarization microscopic image in Fig. 3(b). It is known that collagen in rat-tail tendon consists of three parallel intertwined, polar helices. This non-central-symmetric structure makes it very efficient for second-harmonic generation.[9,11] In this study, rat-tail tendon was removed from thawed rat-tails and stored in phosphate-buffered saline solution for several minutes. A 10-mm-long section was cut from the tendon and put in a sealed glass chamber to ensure sample moisturization.

A microscope objective was used to focus the beam onto the specimen. The average laser power was 80 mW at the sample site. Typical energy per pulse was approximately 1 nJ with energy density of 0.05–0.07 J/cm^2, which is much less than the tissue damage threshold in the range of 0.5–1.0 J/cm^2.[15] When the optical path length difference between the sample and reference arms is within the coherence length of the wave, the SH interference can be detected. The interference signal was demodulated by a lock-in amplifier and used for image construction. Figure 3(a) shows SH-OCT images of the rat-tail tendon obtained with a 0.25-μm-scanning resolution. The image shows the collagen fibrils organization within a 100×50 μm area. As the tension-bearing element in the tendon, collagen appears in clearly defined, parallel, cable-like, and slightly wavy bundles. In this image, highly organized collagen fiber bundles (fascicles) oriented in the same direction can be visualized. Because of the cross-sectioning nature of OCT, collagen fiber bundles localized at different imaging planes parallel to the axial direction exhibit different thicknesses as projected into this image. The transverse and axial resolutions of this image are 1.9 and 4.2 μm, respectively, as determined by the Gaussian beam waist diameter at the focus and coherence length of SH wave.

Understanding the origin of the backscattered SHG signal from the sample is important because in the coherent process of SHG, the majority of the second-harmonic wave copropagates with the excitation laser beam. In highly scattering thick tissues such as tendons, bones, and muscles, the SHG signals detected in the backward direction are mostly from the backscattering of the forward-generated SHG signals. These backscattered SHG signals are collected by the same excitation objective and are particularly important for thick tissues and *in vivo* clinical applications.

The BBO crystal used in the reference arm has a thickness of 0.1 mm and is oriented for type-I phase matching. For SH wavelength conversion of a broadband laser source using a nonlinear crystal, spectrum narrowing effect induced by the crystal dispersion must be considered. Because the spectral width of the SH wave in a bulk of nonlinear crystal is limited by the crystal thickness,[16] the nonlinear crystal has to be made very thin to accommodate for the large bandwidth of a fundamental laser spectrum. The BBO crystal also works as the polarization selector for the SH interference. When the crystal is followed by another quarter wave plate designed for the SH wavelength, the polarization plane of SH wave in the reference arm can be rotated to match that from the sample to produce polarization selective SH-OCT images.

Collagen is the predominant structural protein in most biological tissues, as well as an efficient source of SHG. Modifications of the collagen fibrillar matrix structure are associated with various physiologic processes, such as wound healing, aging, diabetes, and cancer. Therefore, SHG is very promising as a sensitive probe in tissue morphology and physiology studies. OCT has proven to be successful for endoscopic imaging inside bodies of living animals and human patients.[17] With the development of microstructure fibers that support femtosecond laser pulses,[18] SH-OCT has the potential to be implemented with fiber optics and adapted for *in vivo* endoscopic applications.

In summary, we have developed a high-resolution SH-OCT system and applied it to image biological tissues. Structural information about collagen fibrils organization in rat-tail tendon has been revealed in the recorded images. This technique may offer several distinct advantages for imaging ordered, or partially ordered, biological tissues. First, the SHG signal from tissue is a very sensitive indicator of tissue structure and local symmetry changes, and serves as a unique contrast mechanism in optical tomographic imaging. Second, coherence gating extends the capability of high-resolution detection of SHG signals since signals arising out of focal volume can be further rejected. Third, decoupled axial and transverse scans enable two-dimensional tomographic imaging of a sample with only one dimension scanning of the probing beam, which is essential for *in vivo* endoscopic applications.

This work was supported by research grants from the National Science Foundation (BES-86924), National Institutes of Health (EB-00255, NCI-91717, RR-01192), and the Air Force Office of Science Research (FA9550-04-1-0101). Institutional support from the Beckman Laser Institute Endowment is also gratefully acknowledged.

[1] D. Huang, E. A. Swanson, C. P. Lin, J. S. Schuman, W. G. Stinson, W. Chang, M. R. Hee, T. Flotte, K. Gregory, C. A. Puliafito, and J. G. Fujimoto, Science **254**, 1178 (1991).
[2] A. F. Fercher, W. Drexler, C. K. Hitzenberger, and T. Lasser, Rep. Prog. Phys. **66**, 239 (2003).
[3] Z. Chen, T. E. Milner, D. Dave, and J. S. Nelson, Opt. Lett. **22**, 64 (1997).
[4] J. F. de Boer, T. E. Milner, and J. S. Nelson, Opt. Lett. **24**, 300 (1999).
[5] U. Morgner, W. Drexler, F. X. Kärtner, X. D. Li, C. Pitris, E. P. Ippen, and J. G. Fujimoto, Opt. Lett. **25**, 111 (2000).
[6] T. M. Lee, A. L. Oldenburg, S. Sitafalwalla, D. L. Marks, W. Luo, F. J. Toublan, K. S. Suslick, and S. A. Boppart, Opt. Lett. **28**, 1546 (2003).
[7] Y. Jiang, I. Tomov, Y. Wang, and Z. Chen, Opt. Lett. **29**, 1090 (2004).
[8] S. Yazdanfar, L. H. Laiho, and P. T. C. So, Opt. Express **12**, 2739 (2004).
[9] I. Freund and M. Deutsch, Opt. Lett. **11**, 94 (1986).
[10] A. Zoumi, A Yeh, and B. J. Tromberg, Proc. Natl. Acad. Sci. U.S.A. **99**, 11014 (2002).
[11] W. R. Zipfel, R. M. Williams, R. Christie, A. Y. Nikitin, B. T. Hyman, and W. W. Webb, Proc. Natl. Acad. Sci. U.S.A. **100**, 7075 (2003).
[12] E. Brown, T. McKee, E. diTomaso, A. Pluen, B. Seed, Y. Boucher, and R. K. Jain, Nat. Med. (N.Y.) **9**, 796 (2003).
[13] D. A. Dombeck, M. Blanchard-Desce, and W. W. Webb, J. Neurosci. **24**, 999 (2004).
[14] D. A. D. Parry and A. S. Craig, Biopolymers **17**, 843 (1978).
[15] B. M. Kim, J. Eichler, K. M. Reiser, A. M. Rubenchik, and L. B. Da Silva, Lasers Surg. Med. **27**, 329 (2000).
[16] Y. R. Shen, *The Principles of Nonlinear Optics* (Wiley, New York, 1984), Chap. 6, pp.71–73.
[17] G. J. Tearney, M. E. Brezinski, B. E. Bouma, S. A. Boppart, C. Pitris, J. F. Southern, and J. G. Fujimoto, Science **276**, 2037 (1997).
[18] D. G. Ouzounov, F. R. Ahmad, D. Muller, N. Venkataraman, M. T. Gallagher, M. G. Thomas, J. Silcox, K. W. Koch, and A. L. Gaeta, Science **301**, 1702 (2003).